The speed of a tube wave

A. N. Norris
Rutgers University, Department of Mechanics and Materials Science, P. O. Box 909, Piscataway, New Jersey 08855-0909

(Received 10 July 1989; accepted for publication 25 September 1989)

The low-frequency tube wave speed is given explicitly for a variety of borehole environments. The presence of a logging tool, the effects of casing, and bore eccentricity are considered. The results are all relatively simple and indicate that the speed decreases in the presence of a tool or borehole eccentricity. The speed increases in the presence of casing as long as the casing shear modulus exceeds that of the formation.

PACS numbers: 43.20.Mv

INTRODUCTION

The subject of the present paper is the low-frequency speed of the fundamental mode in a fluid-filled cylindrical hole in an elastic matrix. This wave is known in the geophysics community as the tube wave, and the hole is referred to as the bore. At very low frequencies, the other guided modes are evanescent, and the tube wave is of major significance as a carrier of acoustic energy. The tube wave speed for a circular bore is known to reduce to $v = v_B(1 + K_B/\mu_F)^{-1/2}$, where v_B is the acoustic sound speed in the borehole fluid, K_B is the fluid bulk modulus, and μ_F is the shear modulus of the elastic formation surrounding the hole. This expression was deduced by Biot[1] from the low-frequency asymptotic expansion of the Stoneley wave root to the exact dispersion relation.

A simpler and more appealing derivation of Biot's result was provided by White,[2] who used a quasistatic analysis. This assumes the frequency is low enough that the deformation in the fluid and formation can be considered statically. The same method is generalized here to consider more complicated borehole configurations for which the fully dynamic dispersion equation could not be found in a closed form. In each case considered, the formation is an isotropic elastic solid and the bore is cylindrical.

We first look at the effect of a logging tool on the wave speed. Numerical simulations of acoustic signals in a borehole containing a tool[3] indicate the speed is reduced by the tool's presence. The same conclusion follows from the simple analytical results below. White[2] extended his quasistatic analysis to include the presence of concentric borehole casing in a circular bore. However, he only considered lubricated contact between the casings and formation, and then only for casings much more rigid than the formation. The more general results presented here include the possibility of no-slip conditions as well as lubricated contact. Results are also derived for the tube wave speed in an eccentric bore, i.e., one which is not circular but is still cylindrical. No attempt is made here to discuss the effects of formation permeability on the tube wave speed as this topic has been treated adequately elsewhere.[4]

Our results are given in the next section, and their derivation is summarized in Sec. II.

I. SUMMARY OF RESULTS

The low-frequency tube wave speed may generally be written

$$v = (K^*/\rho_B)^{1/2}, \tag{1}$$

where ρ_B is the mass density of the borehole fluid, the effective bulk modulus K^* is

$$\frac{1}{K^*} = \frac{1}{K_B} + \frac{1}{1-f}\left(\frac{1}{M_F} + \frac{f}{M_T}\right), \tag{2}$$

where K_B is the bulk modulus of the borehole fluid, f is the volume fraction the tool occupies in the borehole (see Fig. 1), and M_F and M_T are moduli that depend upon the formation and tool, respectively. The low-frequency results do not require that the tool be concentric with the borehole, only that their axes be parallel.

A. Tool modulus

The logging tool is modeled as an annular elastic shell of shear modulus μ_T and Poisson's ratio ν_T. The interior surface of the shell is assumed to be traction-free; i.e., the acoustic impedance of the inner region is much less than that of the shell. The effective modulus is

$$M_T = \mu_T\{(1 - f_T)/[f_T + (1 - \nu_T)/(1 + \nu_T)]\}, \tag{3}$$

where f_T is the volume fraction of the inner part of the tool. A solid tool corresponds to $f_T = 0$. It is obvious from Eq. (2) that $\partial K^*/\partial f < 0$, and thus the tube wave speed is always diminished in the presence of the tool. Generally, unless the tool is a very thin shell ($f_T \approx 1$), the modulus M_T is of the same order as μ_T, which is typically that of a metal. Thus

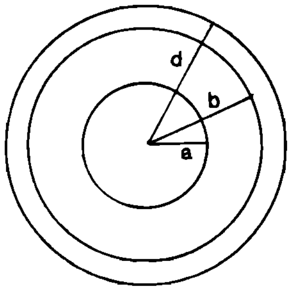

FIG. 1. Schematic of the tool in a circular cased borehole. The tool volume fraction is $f = a^2/b^2$, and the casing volume fraction is $f_C = 1 - b^2/d^2$.

$M_T \gg M_F$ and so the major effect of the tool is to modify the modulus K^* through the volume term $(1-f)^{-1}$ in Eq. (2), i.e., to a good approximation,

$$\frac{1}{K^*} \approx \frac{1}{K_B} + \frac{1}{(1-f)M_F}. \tag{4}$$

B. Formation modulus: Effects of casing

For a homogeneous isotropic solid formation of shear modulus μ_F surrounding a circular bore, it is well known[11] that

$$M_F = \mu_F. \tag{5}$$

This result is modified if the borehole is cased by a concentric isotropically elastic annular shell that is fitted tight against the formation. Let the casing have shear modulus μ_C and Poisson's ratio ν_C. If the inner radius of the casing is b and the outer radius d, define the volume fraction the casing occupies as $f_C = 1 - b^2/d^2$; see Fig. 1. Then,

$$M_F = \mu_F\left(\frac{1-\nu_C + (f_C/2)(\mu_C/\mu_F - 1)(1-\beta\nu_C^2)}{1-\nu_C + (f_C/2)(\mu_F/\mu_C - 1)(1-2\nu_C+\beta\nu_C^2)}\right), \tag{6}$$

where β is a parameter that defines the state of contact between the casing and formation. The two limits of interest are no-slip, $\beta = 0$, when the casing is restrained from moving in the axial direction relative to the formation, and lubricated contact, $\beta = 1$, in which case such motion is allowed. Usually, the casing is put in place for the very reason that it is far more rigid than the formation, $\mu_C \gg \mu_F$, which implies that $M_F > \mu_F$, independently of β, and thus the tube wave speed is increased by the casing. It can easily be shown that M_F and hence the wave speed decreases as the contact becomes more lubricated, i.e., as β increases from 0 to 1.

When the casing thickness h is much less than the bore radius d, then $f_C \sim 2h/d$, and M_F of Eq. (6) can be approximated accordingly. If the casing is also far more rigid than formation, $\mu_C \gg \mu_F$, then,

$$M_F \approx \mu_F + (h/2d)E_C[(1-\beta\nu_C^2)/(1-\nu_C^2)], \tag{7}$$

where $E_C = 2\mu_C(1+\nu_C)$ is the Young's modulus of the casing. The approximation (7) has been given by White[2] for lubricated contact, $\beta = 1$. The two limits of $\beta = 0$ and $\beta = 1$ are also known as the tethered and untethered cases, respectively.[5] This reference contains an interesting discussion of the relevance of tube waves in biological pulse propagation phenomena.

C. Formation modulus: Effects of bore eccentricity

Holes of arbitrary shape can be considered using the methods of Zimmerman,[6] who discussed the compressibility of two-dimensional cavities in elastic solids. Let $w(\zeta)$ be the complex mapping function that maps the interior of the unit circle in the complex ζ plane into the exterior of the region defined by the hole in the complex z plane, where $z = x + iy = w(\zeta)$. In particular, $w(\zeta)$ may be expressed in the form

$$w(\zeta) = \zeta^{-1} + \sum_{n=1}^{\infty} a_n \zeta^n, \tag{8}$$

where a_n, $n = 1,2,3,\ldots$, are complex numbers specified by the shape of the hole. The circular hole corresponds to $w = \zeta^{-1}$, and an ellipse of aspect ratio α is given by $a_1 = (1-\alpha)/(1+\alpha)$, $a_n = 0$, $n > 1$. Define σ, $0 \leqslant \sigma \leqslant 1$, by

$$\sigma = \sum_{n=1}^{\infty} n|a_n|^2; \tag{9}$$

then the formation modulus is

$$M_F = \mu_F\{1 + 4(1-\nu_F)/(\sigma^{-1} - 1)\}^{-1}. \tag{10}$$

It is clear from Eq. (10) that the modulus M_F for the circular hole is greater than that for any other shape,[6] and therefore the tube wave speed is fastest in a circular bore. When the hole is almost circular, σ is small, and $M_F = \mu_F[1 - 4(1-\nu_p)\sigma + O(\sigma^2)]$. For instance, $\sigma = (1-\alpha)^2/(1+\alpha)^2$ for an ellipse of aspect ratio α, and so as $\alpha \to 1$, $M_F \approx \mu_F[1 - (1-\nu_F)(1-\alpha)^2]$. Shapes that are quite distinct from circular, such as the hypotrochoid, have been discussed by Zimmerman.[6] Equilateral, s-sided polygons may be considered by the two-term Schwartz–Christoffel approximation to the mapping function,

$$w(\zeta) = \zeta^{-1} + 2/[s(s-1)]\zeta^{s-1}, \tag{11}$$

for which

$$\sigma^{-1} = (s^2/4)(s-1). \tag{12}$$

Thus the pseudosquare given by (11) with $s = 4$ has $\sigma^{-1} = 12$, while the exact value that follows from the mapping function for the square[6] is $\sigma^{-1} = 11.62$.

D. Examples

Consider a water-filled bore in Teapot sandstone,[4] for which $K_B = 2.25$ GPa, $v_B = 1500$ m/s, $\mu_F = 6.45$ GPa, and $\nu_F = 0.20$. Then, the tube wave speed for the simple circular bore is 1292 m/s, and, for a square bore $v = 1244$ m/s. Suppose the circular bore is cased with steel, $\mu_C = 79.4$ GPa, $\nu_C = 0.29$, such that the casing is 1 cm thick with outer radius $d = 10$ cm. The tube wave speed then follows from Eq. (6) as 1410 m/s for perfectly bonded contact, and 1407 m/s for lubricated contact. The corresponding approximate speeds according to Eq. (7) are 1413 and 1408 m/s, respectively. Next, consider the same circular bore of radius $d = 10$ cm with no casing but which contains a steel tool in the form of a cylindrical shell of thickness 2 cm and exterior radius 6 cm. The tube wave speed follows from Eq. (3) as 1201 m/s, and the approximation of Eq. (4) gives a speed of 1207 m/s.

As expected, the speed is increased relative to that of the simple circular bore when the casing is present. On the other hand, bore eccentricity and the presence of a tool result in a slower speed. Suppose, however, that the tool and casing are both present, then the speed for a well-bonded casing is 1336 m/s. In this case, the decrease in speed due to the tool is more than made up for by the increase caused by the stiffening effect of the casing.

II. DERIVATION OF THE RESULTS

The general method of solution is a simple extension of White's (p. 146 of Ref. 2) quasistatic analysis. The acoustic pressure p_B and axial displacement u_z in the borehole fluid are functions of time and the axial coordinate z only. The axial force balance in a thin slice of length Δz of the fluid is

$$\rho_B \frac{\partial^2 u_z}{\partial t^2} V = \frac{-\partial p_B}{\partial z} V, \tag{13}$$

where ρ_B is the fluid density,

$$V = A\Delta z, \tag{14}$$

and A is the cross-sectional area of the bore that is occupied by fluid. Thus $A = A_B - A_T$, where A_T is the cross-sectional area of the tool, and A_B the area inside the casing, or inside the formation in the absence of casing. The fraction f in Eq. (2) is A_T/A_B. The fluid pressure is

$$p_B = -K_B(\Delta V/V), \tag{15}$$

where K_B is the borehole fluid bulk modulus,

$$\Delta V = \left(A \frac{\partial u_z}{\partial z} + \Delta A\right)\Delta z, \tag{16}$$

and ΔA is the static change in the area A due to the pressure p_B. Thus

$$\Delta A = \int_{C_B} u_n \, ds + \int_{C_T} u_n \, ds, \tag{17}$$

where C_T is the perimeter of the tool cross section, C_B the outer perimeter of the bore cross section, and u_n is the normal fluid displacement in the direction away from the fluid. Combining Eqs. (14)–(17) gives

$$p_B = -K^* \frac{\partial u_z}{\partial z}, \tag{18}$$

where K^* is defined in Eq. (2), and

$$\frac{1}{M_F} = \frac{1}{p_B A_B} \int_{C_B} u_n \, ds, \tag{19}$$

$$\frac{1}{M_T} = \frac{1}{p_B A_T} \int_{C_T} u_n \, ds. \tag{20}$$

The modulus M_T follows from Eq. (20) by solving the problem of a tool subject to a uniform pressure p_B on its outer surface. The tool is modeled as a homogeneous elastic circular shell, and its interior surface is assumed to be pressure free. The uniform displacement u_n then follows by solving a simple plane stress problem in static elasticity.[7]

The determination of the modulus M_F requires solving a plane problem for an elastic material exterior to C_B subject to uniform pressure p_B on C_B. When the casing is present the problem becomes that of a circular hole with a lining of uniform thickness. The condition at the interface between the casing and formation is that the radial stress and displacement are continuous. The solution is radially symmetric so that there is no shear stress at the interface. The no-slip contact condition [$\beta = 0$ in Eq. (6)], requires solving plane *strain* problems in both the casing and formation. However, for lubricated contact ($\beta - 1$), the casing can undergo axial displacement, in which case the problem is one of plane strain in the formation but plane *stress* in the casing.

The results for the modulus M_F of an arbitrarily shaped hole follow from the work of Zimmerman[6] by noting that $M_F^{-1} = C_{pp}$, where in the notation of Ref. 6, C_{pp} is the compressibility of the cavity with respect to the inner or pore pressure. Zimmerman[6] showed, using complex variable methods developed by Muskhelishvili[8] and Sokolnikoff,[9] that

$$C_{pp} = (1/\mu_F)[(1 + \chi\sigma)/(1 - \sigma)], \tag{21}$$

where σ is defined in Eq. (9) and $\chi = 3 - 4\nu_F$ for plane strain, $\chi = (3 - \nu_F)/(1 + \nu_F)$ for plane stress. The borehole problem is one of plane strain and so we obtain Eq. (10) for M_F. Finally, we note that one can also define different measures of compressibility for the same hole, if, for instance, the confining pressure is applied at infinity rather than inside the hole. The distinctions between these various compressibilities is discussed extensively by Zimmerman[6] and Zimmerman *et al.*[10]

III. CONCLUSIONS

Relatively simple and explicit formulas have been given for the low-frequency tube wave speed, including new results for the speed in the presence of a tool and when the bore is noncircular. These show that the speed always decreases in the presence of a tool, and for a given tool size it decreases as the tool becomes more elastically compliant. However, when the tool is relatively rigid, its main influence is to reduce the effective cross-sectional area of the bore. The tube wave speed for the circular bore is greater than the speed for any other shaped hole. The only effect that can increase the tube wave speed is the presence of a casing stiffer than the formation, and the increase in speed is greatest when the casing is perfectly bonded, but is slightly diminished when the contact between the formation and the casing is lubricated. None of these conclusions is surprising or unexpected, but the simplicity of the associated expressions make them very suitable for estimating the low-frequency tube wave speed in complicated environments where exact analytical techniques are of little or no use and numerical simulation is too cumbersome.

ACKNOWLEDGMENTS

This work was supported in part by Exxon Research and Engineering Company, and also by the National Science Foundation through Grant No. MSM85-16256.

[1] M. A. Biot, "Propagation of elastic waves in a cylindrical bore containing a fluid," J. Appl. Phys. 23, 997–1005 (1952).

[2] J. E. White, *Underground Sound* (Elsevier, New York, 1983).

[3] C. H. Cheng and M. N. Toksoz, "Elastic wave propagation in a fluid-filled borehole and synthetic acoustic logs," Geophysics **46**, 1042–1053 (1981).

[4] A. N. Norris, "Stoneley-wave attenuation and dispersion in permeable formations," Geophysics **54**, 330–341 (1989).

[5]J. Lighthill, *Waves in Fluids* (Cambridge U.P., Cambridge, England, 1980), p. 98.
[6]R. W. Zimmerman. "Compressibility of two-dimensional cavities of various shapes," J. Appl. Mech. **108**, 500–504 (1986).
[7]S. Timoshenko and J. N. Goodier, *Theory of Elasticity, 3rd Ed.* (McGraw-Hill, New York, 1970).
[8]N. I. Muskhelishvili, *Some Basic Problems of the Mathematical Theory of Elasticity, 4th Ed.* (Noordhoff, Groningen, 1963).
[9]I. S. Sokolnikoff, *Mathematical Theory of Elasticity, 2nd Ed.* (McGraw-Hill, New York, 1956).
[10]R. W. Zimmerman, W. H. Somerton, and M. S. King, "Compressibility of porous rocks," J. Geophys. Res. **91**, 12765–12777 (1986).

Underwater audiogram of a Hawaiian monk seal (*Monachus schauinslandi*)

Jeanette Thomas, Patrick Moore, Reid Withrow,[a] and Mark Stoermer
Naval Ocean Systems Center, Kailua, Hawaii 96734

(Received 15 January 1989; accepted for publication 22 September 1989)

Underwater audiograms are available for a few pinnipeds from the families otariidae and phocidae, but little is known about hearing abilities in the monachid seals. A young male Hawaiian monk seal (*Monachus schauinslandi*) was trained at Sea Life Park on Oahu, Hawaii for an underwater hearing test using a go/no-go response paradigm. Over a 6-month period, auditory thresholds from 2 to 48 kHz were measured using an up/down staircase psychometric technique. The resulting audiogram shows a somewhat narrower hearing range than for other pinnipeds. The monk seal's hearing was most sensitive (20 dB above maximum sensitivity) between 12 and 28 kHz. Below 8 kHz, the Hawaiian monk seal's hearing was less sensitive than other pinnipeds measured. High-frequency sensitivity dropped off sharply above 30 kHz, as has been reported for other otariids, *Callorhinus* and *Zalophus*. Phocid seals, *Phoca hispida*, *P. groenlandica*, and *P. vitulina*, have a broader hearing range with the upper limit near 60 kHz.

PACS numbers: 43.66.Cb, 43.80.Lb, 43.66.Gf [NFV]

INTRODUCTION

Hawaiian monk seals (*Monachus schauinslandi*) are largely solitary animals, congregating at traditional beaches on the outer Hawaiian island chain during a short breeding season (Johnson *et al.*, 1982). They are an endangered species because of high mortality of pups and a surplus of adult males. However, National Marine Fisheries Service has a rehabilitation program for captive pups (Gilmartin, 1983; Gilmartin and Gerrodette, 1986; Gilmartin *et al.*, 1986). One of these captive male pups was the subject for our study.

Little is known about the sensory abilities of the seclusive Hawaiian monk seal. They produce a few vocalizations while hauled out on the beach. Although there have been a few attempts to record their vocalizations at sea, none has been reported (Gilmartin, personal communcation).

Antarctic seals, like the Weddell seal (*Leptonychotes weddelli*), the leopard seal (*Hydrurga leptonyx*), and the crabeater seal (*Lobodon carcinophagus*), are members of the family Monachidae. Hearing abilities in these seals also are unknown, but, in contrast to the Hawaiian monk seal, they are highly vocal (Thomas and Kuechle, 1982; Stirling and Siniff, 1979). A report by Thomas *et al.* (1982) indicates that leopard seals produce very high-frequency vocalizations, up to 130 kHz. This observation led us to suspect that monachid seals might have a broader high-frequency hearing range than other pinnipeds. Our objectives were to measure the underwater hearing ability of a Hawaiian monk seal and compare our results with audiograms from other pinnipeds.

[a]At Waikiki Aquarium, Honolulu, Hawaii 96815.

I. METHODS

A. Subject

A 3-year-old, male Hawaiian monk seal, "Maka," was our test subject. At the end of the study, this animal weighed 120 kg, was about 1.6 m long, and had been in captivity for 2 years. The seal lived in a quiet test pool, with only a skimmer filter system that did not require mechanical pumps. This untrained animal learned the testing paradigm in about 3 months We tested the seal's hearing twice per day from December 1987 to February 1988. The animal received a daily ration of 3 kg of herring during the tests.

B. Apparatus

We conducted the study in a 6.1-m-diam × 1.2-m-deep fiberglass pool in a quiet back holding area at Sea Life Park on Oahu, Hawaii. The equipment setup in this pool is shown in Fig. 1. A slatted redwood platform (A in Fig. 1) served as a haulout site for the animal, a stage for the trainer, and support for the signal projection equipment. A cage (B in Fig. 1) attached to the pool provided a holding area for the seal during equipment installation and removal. The seal's test station (C in Fig. 1) was a headstand with a short rim shaped to the contour of the lower jaw. The seal's ears and face were unobstructed from the projector's sound field. The headstand was attached to the pool bottom by three glass-